Proceedings of the 12th International Congress on the Cement Chemistry
Montréal, Canada ,8-13 July, 2007

# Progress in mathematical modeling using $C^{em}$Quant software for quantitative phase analysis of Portland cement

B. Feret[1], V.J.F. Feret[1]
[1]*BF Simulation, Jonquière, Quebec, Canada*

## Abstract

At present there are several known methods to determine mineralogy of clinker cement: Bogue, microscopy, ASTM C150, Rietveld-XRD and $C^{em}$Quant. Each has certain advantages and disadvantages. The first commercial version of the $C^{em}$Quant software appeared in 1998, followed by a publication [1]. In this first $C^{em}$Quant version up to 17 constituents, including CaO, $SiO_2$, $Al_2O_3$, $Fe_2O_3$, $SO_3$, MgO, $TiO_2$, $Mn_2O_3$, SrO, $Na_2O$, $K_2O$, $P_2O_5$ and loss of mass at 1000 °C made up the input data. Using a novel mathematical modeling approach, the input constituents were distributed among pre-selected mineral phases in such a way that the input and output mass balances were matched. However, to obtain the most accurate output data the concentrations of calcite and gypsum were required, which was not convenient.

A new version of $C^{em}$Quant has been developed that compensates for past inefficiencies and makes the software much more practical to use. The input data was modified to include additional loss of mass concentration determined at 480 °C. Using either a manual or automatic TGA device this additional measurement does not represent a problem. The phases automatically quantified by $C^{em}$Quant are: alite, belite, aluminate, ferrite, aphthialite, gypsum, bassanite, lime, calcite, periclase, langbeinite, thenardite, arcanite, C4AMn, anhydrite and perovskite. Particularly useful is the new software's ability to precisely estimate the amount of gypsum and bassanite in Portland cement.

The software deals very effectively with both major and secondary phases, including those that are associated with alkali elements; they are almost impossible to quantify by other methods. In addition, it is possible to model the stoichiometry of ferrite for R&D or process control purposes. Calculation results for selected standard samples are given as example. It is believed that the current $C^{em}$Quant software yields the most accurate phase concentrations of clinker and Portland cement. The $C^{em}$Quant software could be considered as a cost-effective alternative to established methods of clinker and Portland cement phase analysis.

Keywords: clinker, Portland cement; phase composition determination; mathematical modeling; X-ray diffraction, X-ray fluorescence, TGA, $C^{em}$Quant

## 1. Introduction

The quantitative phase analysis of clinker and Portland cement has always been of considerable interest to the plants and cement users. Steady increase in the energy cost in the recent years made this interest even more important. Despite a visible progress in cement phase quantification demonstrated by Rietveld-XRD analysis the several decades old Bogue calculation continues to be used. Very many cement manufacturers and users are simply not equipped with the X-ray diffraction technology in their laboratories. Even if the Rietveld-XRD technology finds its way into the laboratory the associated effort, complexity (due to both sample preparation and analysis) and expenses are not negligible. Generally, the X-ray fluorescence spectrometers are much more frequently encountered in cement laboratories than X-ray diffractometers. In this light calculation of the cement phase composition using $C^{em}$Quant and employing sample's elemental concentrations and loss of mass appears to be an attractive alternative to X-ray diffraction. The first generation $C^{em}$Quant software appeared in 1998 and a corresponding paper followed [1]. In that first $C^{em}$Quant version, up to 17 constituents, including CaO, $SiO_2$, $Al_2O_3$, $Fe_2O_3$, $SO_3$, MgO, $TiO_2$, $Mn_2O_3$, SrO, $Na_2O$, $K_2O$, $P_2O_5$ and loss of mass at 1000 °C (LOM) made up the input data. Using a novel mathematical modeling approach, the input constituents were distributed among pre-selected mineral phases in such a way that the input and output mass balances were matched. However, to obtain the most accurate output data the concentrations of calcite and gypsum were required, which was not practical. The second-generation $C^{em}$Quant was developed that compensates for past inefficiencies and makes the software much more attractive to the user. The objective of this paper is to describe the new software and present selected results obtained with it.

## 2. The $C^{em}$Quant concept

Although the $C^{em}$Quant fundamentals have not been changed, several important modifications of the first-generation algorithm were made. The input data was modified to include additional loss of mass concentration determined at 480 °C ($LOM_1$). Employing either manual (muffle furnace) or automatic TGA device this additional measurement does not represent a problem. The LOM at 1000 °C continues to be required with the new software as well.

The input data of the second-generation $C^{em}$Quant consists of constituents as follows: CaO, $SiO_2$, $Al_2O_3$, $Fe_2O_3$, $SO_3$, MgO, $TiO_2$, $Mn_2O_3$, SrO, $Na_2O$, $K_2O$, $P_2O_5$, LOM, and $LOM_1$. Only the first six oxides are absolutely required to run the software. However, minor element oxides and LOM are essential if full mineralogy is to be calculated and a high accuracy output data is to be obtained. The LOM data is not required if it is known to be at low content (<0.3%). The $LOM_1$ concentration is only required for analysis of Portland cement and it is not required in the case of clinker phase analysis. A sample composition corresponding to clinker and Portland cement is calculated, provided that the input constituents fall within the concentration ranges listed in Table 1. Another condition that needs to be met is: $97.5\% < \text{TOTAL} < 102.5\%$, where TOTAL is the sum of the input concentrations. Obviously, the more accurate the input concentrations are the more accurately the output phases are determined.

Table 1
CemQuant input data: elemental composition (expressed as oxides)

| **Input Data** | **Composition Limit (%)** | |
|---|---|---|
| | **Low** | **High** |
| CaO | 50.0 | 75.0 |
| $SiO_2$ | 16.0 | 26.5 |
| $Al_2O_3$ | 1.2 | 15.0 |
| $Fe_2O_3$ | 0.02 | 20.0 |
| $TiO_2$ | 0 | 2.5 |
| $Mn_2O_3$ | 0 | 1.0 |
| SrO | 0 | 1.0 |
| MgO | 0.02 | 7.0 |
| $Na_2O$ | 0 | 2.0 |
| $K_2O$ | 0 | 2.5 |
| $P_2O_5$ | 0 | 3.0 |
| $SO_3$ | 0 | 7.3 |
| $LOM_1$(480 °C) | 0 | 8.5 |
| LOM (1000 °C) | 0 | 8.5 |

The $C^{em}$Quant concept is based on the assumption that the LOM and the elemental composition of a cement sample would constitute sufficient input data for generation of the phase content. The $C^{em}$Quant algorithm employs generally acknowledged but complex stoichiometry of phases in cement [2], and the mass balance [1-4]. It is assumed that the LOM and the elemental constituents are distributed among pre-selected mineral phases in such a way that the input and output mass balances are matched. Based on the input data presented in Table 1, finding a phase composition solution for a cement specimen is a very unusual task. Almost all major and minor input constituents naturally occur in several output phases. The problem with finding a solution for such a system was that the number of unknowns considerably exceeded the number of known input constituents. Such a system described in the form of a set of algebraic equations does not have a unique (non-zero) solution. Thus, the mass balance equations were solved with the help of mathematical modeling [1, 3], based on Monte Carlo method [5]. This iterative procedure involves the use of random number generators employed to approximate the solution. Uniformly distributed pseudorandom numbers are generated using the multiplicative congruential method between the chosen lower and upper concentration limits. The arithmetic means of all acceptable values aided by an exclusion method give an estimate of the final phase concentrations. Should the lime concentration be known from other independent methods, this can be incorporated and may improve the approximation of the remaining phases.

Table 2 lists phases dealt with in the present version of $C^{em}$Quant and gives their description. The phases quantified by $C^{em}$Quant are: alite, belite, aluminate, ferrite, aphthialite, gypsum, bassanite, lime, calcite, periclase, langbeinite, thenardite, arcanite, C4AMn, anhydrite and perovskite. Compared to the previous software [1], the new second-generation software deals thoroughly and effectively with constituent's solubility. Major substitutions in alite, belite, aluminate and ferrite involve Na, K, Mg and Al. The substitutions may occur in predefined ranges. As a result, gone from the algorithm are three phases that were considered for quantification previously: $KC_8A_3$, $NC_8A_3$ and $KC_{23}S_{12}$. Phases described in Table 2 are automatically selected during simulation runs (by default). However, several user selected secondary phases might be inserted, if justified, to replace those that are currently employed by default. As such, $C^{em}$Quant would allow analysis of unusual phase composition associated with particular raw materials and process conditions.

Among current software options user may settle for default stoichiometry of aluminate and ferrite (decided for every sample by the software) or fix a specific stoichiometry for a research work. A similar possibility exists with respect to choosing the solubility level of MgO. There is also a possibility to consider $TiO_2$ as being associated with perovskite or appearing in connection with $4CaO{\cdot}2FeO{\cdot}TiO_2$. Concentration of $TiO_2$ is usually low. However, occasional elevated $TiO_2$ concentration may have important influence on the phase quantification process and should be taken into account.

Table 2
Phases that are quantified and their description

| Phase | Chemical Formula | Maximum Concentration (%) |
|---|---|---|
| Alite | $(Ca_{1-x-y}Mg_xAl_y)_3\cdot(Si_{1-y}Al_y)O_5$ | 80 |
| Belite | $(Ca_{1-x-y}Mg_xAl_y)_2\cdot(Si_{1-y}Al_y)O_4$ | 45 |
| Aluminate | $(Ca_{1-x-y},K_xNa_y)_3\cdot Al_2O_6$ | 15 |
| Ferrite | $Ca_2(Al_xFe_{1-x})_2O_5$ | 20 |
| Aphthialite | $K_3Na(SO_4)_2$ | 8 |
| Gypsum | $CaSO_4\cdot 2H_2O$ | 9 |
| Bassanite | $CaSO_4\cdot 0.5H_2O$ | 5 |
| Lime | $CaO$ | 3 |
| Calcite | $CaCO_3$ | 8 |
| Periclase | $MgO$ | 8 |
| Langbeinite | $Ca_2K_2(SO_4)_3$ | 5 |
| Thenardite | $Na_2SO_4$ | 5 |
| Arcanite | $K_2SO_4$ | 5 |
| $C_4AMn$ | $Ca_4Al_2Mn_2O_{10}$ | 5 |
| Anhydrite | $CaSO_4$ | 3 |
| Perovskite | $CaTiO_3$ | 4.5 |

Given profound changes in the algorithm the performance of the second-generation software has been improved significantly. Particularly useful is the new software's ability to precisely estimate the amount of gypsum and bassanite generated in the Portland cement grinding process. The software deals very effectively with both major and secondary phases, including those that are associated with alkali elements, which are almost impossible to quantify by other methods. It is believed that current C$^{em}$Quant software yields accurate phase concentrations of clinker and Portland cement and provides the most realistic phase composition for a known input data. Calculation results for selected standard samples are given as example.

## 3. Results

Fifteen international cement reference materials [6] were analyzed using C$^{em}$Quant. Their input concentration data is given in Table 3.

Table 3
Input composition data (%) of cement reference materials

| S. ID | CaO | SiO2 | Al2O3 | Fe2O3 | TiO2 | Mn2O3 | SrO | MgO | Na2O | K2O | P2O5 | SO3 | LOM1 | LOM | Lime |
|---|---|---|---|---|---|---|---|---|---|---|---|---|---|---|---|
| SRM2686 | 63.36 | 22.48 | 4.7 | 3.6 | 0.25 | 0.1 | 0.05 | 4.73 | 0.1 | 0.42 | 0.06 | 0.27 | 999 | 0.16 | 0.3 |
| SRM2687 | 67.2 | 21.43 | 5.53 | 1.98 | 0.27 | 0.04 | 0.11 | 1.48 | 0.14 | 0.72 | 0.29 | 0.83 | 999 | 0.17 | 2.2 |
| SRM2688 | 66.5 | 22.68 | 4.9 | 4.07 | 0.24 | 0.03 | 0.13 | 0.98 | 0.11 | 0.35 | 0.08 | 0.31 | 999 | 0.21 | 0.2 |
| SRM1880 | 63.14 | 19.82 | 5.03 | 2.91 | 0.23 | 0.08 | 0.06 | 2.69 | 0.28 | 0.91 | 0.29 | 3.37 | 999 | 1.38 | 2.3 |
| SRM1884 | 64.01 | 23.19 | 3.31 | 3.3 | 0.16 | 0.11 | 0.048 | 2.32 | 0.13 | 0.51 | 0.12 | 1.67 | 999 | 1.17 | 0.01 |
| SRM1885a | 62.39 | 20.91 | 4.03 | 1.93 | 0.20 | 0.05 | 0.64 | 4.03 | 1.07 | 0.21 | 0.12 | 2.83 | 999 | 1.68 | 2.05 |
| SRM1886a | 67.87 | 22.38 | 3.88 | 0.15 | 0.08 | 0.01 | 0.02 | 1.93 | 0.02 | 0.09 | 0.02 | 2.09 | 999 | 1.56 | 2.16 |
| SRM1887a | 60.90 | 18.64 | 6.20 | 2.86 | 0.27 | 0.12 | 0.32 | 2.84 | 0.48 | 1.10 | 0.31 | 4.62 | 999 | 1.43 | 0.53 |
| SRM1888a | 63.23 | 21.22 | 4.27 | 3.08 | 0.26 | 0.13 | 0.08 | 2.98 | 0.11 | 0.53 | 0.80 | 2.13 | 999 | 1.75 | 0.79 |
| SRM1889 | 65.34 | 20.66 | 3.89 | 1.94 | 0.23 | 0.26 | 0.04 | 0.81 | 0.20 | 0.61 | 0.11 | 2.69 | 999 | 3.28 | 0.58 |
| CCRL141 | 60.93 | 19.07 | 5.68 | 2.45 | 0.26 | 0.08 | 0.29 | 2.55 | 0.35 | 1.05 | 0.27 | 4.55 | 1.0 | 1.84 | 0.41 |
| CCRL142 | 61.16 | 20.33 | 4.62 | 2.74 | 0.21 | 0.15 | 0.29 | 3.99 | 0.25 | 1.10 | 0.18 | 3.42 | 0.26 | 0.99 | 0.81 |
| BCS353 | 64.8 | 20.5 | 3.77 | 4.82 | 0.16 | 0.23 | 0.23 | 2.42 | 0.1 | 0.49 | 0.077 | 2.25 | 999 | 0.13 | 999 |
| BCS354 | 70 | 21.8 | 4.84 | 0.3 | 0.04 | 0.058 | 0.11 | 0.42 | 0.1 | 0.11 | 0.12 | 2.25 | 999 | 0.01 | 999 |
| BCS372 | 65.3 | 20.3 | 5.37 | 3.42 | 0.29 | 0.074 | 0.05 | 1.31 | 0.1 | 0.76 | 0.07 | 2.95 | 999 | 0.01 | 999 |

One of the $C^{em}$Quant features is its ability to estimate free lime. Even if the $LOM_1$ (at 480 °C) and free lime concentrations are not specified for certain samples (marked with *999* in Table 3) $C^{em}$Quant is still able to estimate phase concentrations. However, when the $LOM_1$ and free lime concentrations are experimentally determined the estimation accuracy of most phases (particularly gypsum, calcite, anhydrite and bassanite) improves. Table 4 gives the minimum and maximum phase concentrations obtained using $C^{em}$Quant for the input data in Table 3.

Table 4
Variation range of phase concentrations (%) obtained using $C^{em}$Quant

| | Alite | Beli | Alu | Ferr | Aph | Gyp | Bas | Lim | Cal | Peri | Lang | Ther | Arca | C4AM | Anh | Perov |
|---|---|---|---|---|---|---|---|---|---|---|---|---|---|---|---|---|
| Min | 22.2 | 2.5 | 1.6 | 1 | 0 | 0 | 0 | 0 | 0 | 0 | 0 | 0 | 0 | 0 | 0 | 0.1 |
| Max | 80 | 48.7 | 11.3 | 14.5 | 2.1 | 3.5 | 2.5 | 3 | 3.3 | 3.5 | 0 | 0.2 | 1 | 0.8 | 3.9 | 1.8 |

where: Alite = alite, Beli = belite, Alu = aluminate, Ferr = ferrite, Aph = aphthialite, Gyp = gypsum, Bas = bassanite, Lim = lime, Cal = calcite, Peri = periclase, Lang = langbeinite, Ther = thenardite, Arca = arcanite, C4AM = $Ca_4Al_2Mn_2O_{10}$, Anh = anhydrite, Perov = perovskite.

$C^{em}$Quant estimated alite, belite and ferrite (Fig. 1-3) concentrations were compared with those obtained by the ASTM C150 [7] and NIST [8] methods. Rietveld-XRD results obtained by Taylor at al. [9] and TOPAS [10] methods were also compared.

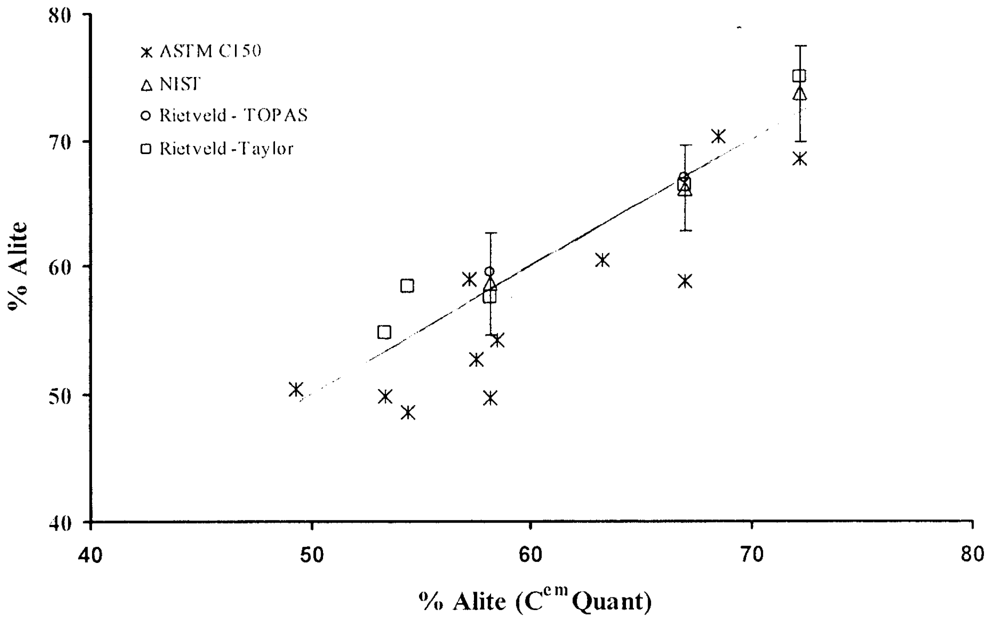

Fig. 1. Correlation graph for alite

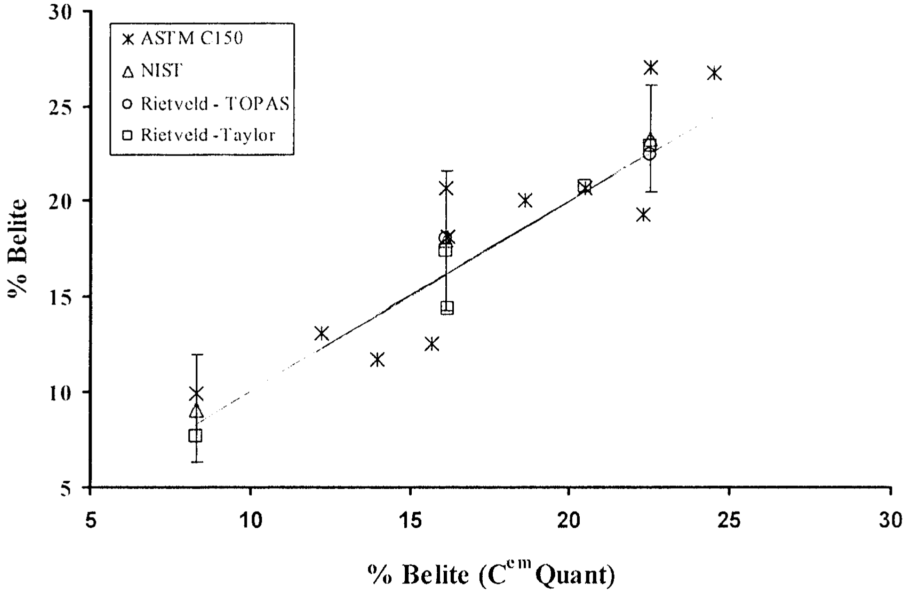

Fig. 2. Correlation graph for belite

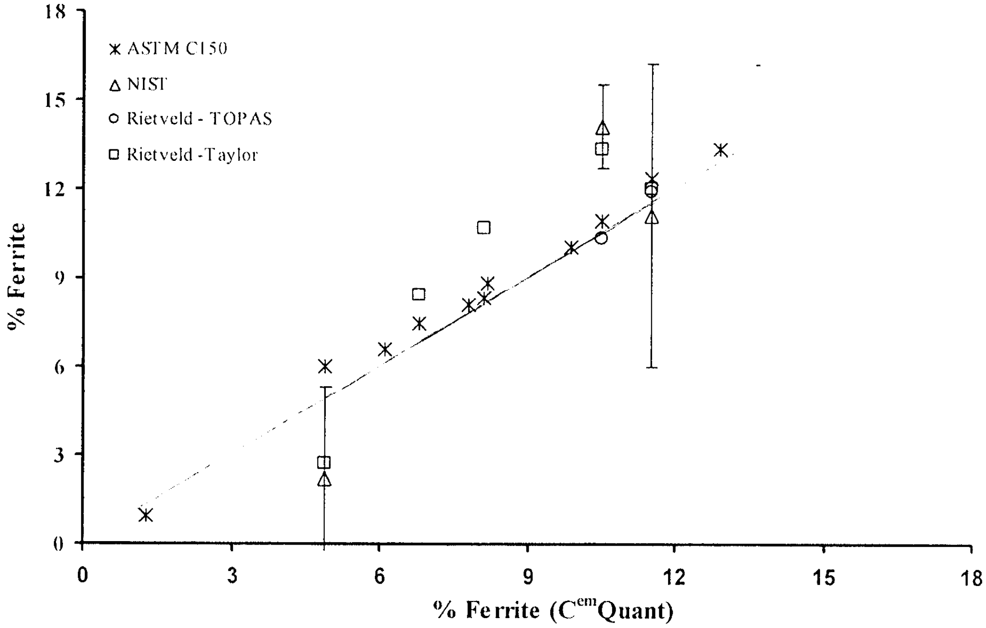

Fig. 3. Correlation graph for ferrite

Figures 1 and 2 show that in comparison with C$^{em}$Quant the ASTM concentrations of alite and belite form scattered points. The C$^{em}$Quant estimated ferrite concentrations (Fig. 3) are in good agreement with those obtained by the ASTM method. The vertical error bars in Fig. 1- 3 reflect the NIST estimation errors. Absolute average differences between C$^{em}$Quant and ASTM estimates are 4.9 % for alite, 3.2% for belite and 0.5% for ferrite. The extreme ferrite concentrations obtained from both methods agree well. The Rietveld-XRD (TOPAS, Taylor) concentrations for alite and belite compare well with C$^{em}$Quant data in this work. In general, the Rietveld-XRD phase concentrations for major phases such as alite, belite and ferrite may appear higher than those obtained from C$^{em}$Quant. This is due to XRD's known difficulty with quantification of the secondary phases and with the amorphous content. Rietveld-XRD and also microscopic methods normalize output data to 100% [11, 12]; this increases concentrations of the major phases.

Additional test was carried out to compare concentrations of gypsum and bassanite estimated by C$^{em}$Quant and obtained by Rietveld-XRD [13, 14] and DSC [15]. The LOM$_1$ concentrations for C$^{em}$Quant runs were calculated from known (experimental) gypsum and bassanite concentrations. Figires 3 and 4 show a good comparison of C$^{em}$Quant calculated and the experimental concentrations of gypsum and bassanite. Absolute average differences between the C$^{em}$Quant estimates and the experimental values are 0.2 % for gypsum and 0.5 % for bassanite.

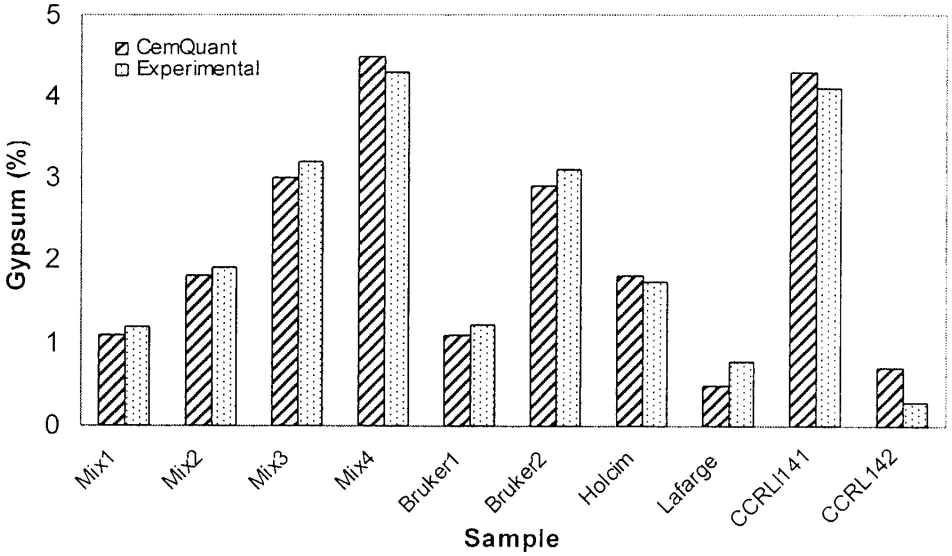

Fig. 4. Comparison of $C^{em}$Quant calculated and experimental concentrations of gypsum

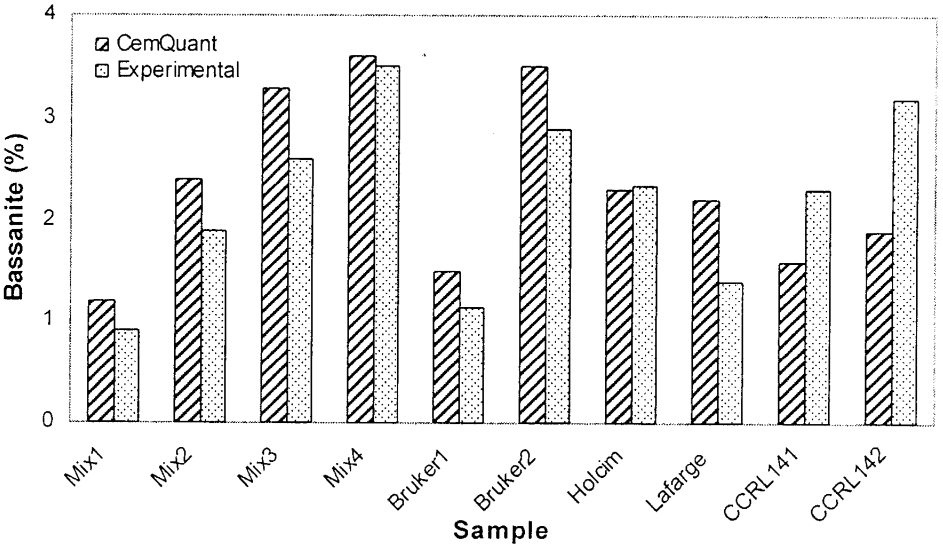

Fig. 5. Comparison of $C^{em}$Quant calculated and experimental concentrations of bassanite

## 4. Discussion

It is difficult to compare phase quantification results obtained using different methods. This is because there is no independent measurement or verification possible, which would yield "true" phase composition data. Most secondary or trace phases cannot be quantified at all when employing existing methodologies such as XRD-calibration, XRD-Rietveld, microscopy and wet chemistry (WCh). This is because the respective limits of detection are simply too high.

C$^{em}$Quant's algorithm takes care of the secondary constituents and their solubility. Moreover, these constituents help determine occurrence or absence of certain phases. Direct Bogue method is inadequate because it does not take secondary and trace elements into consideration. On the other hand, Rietveld-XRD based phase quantification employs a diffractogram, which represents crystallographic reality that is far from being perfect. XRD misses some crucial secondary phases due to their relatively high limit of detection. For example, aphthialite, calcite, anhydrite or arcanite need to occur at concentrations exceeding 0.3 – 0.5% to become quantifiable. The XRD limit of detection of the secondary phases strongly depends on the $Fe_2O_3$ content. Free lime content below 0.7% by mass lies below the limit of detection of the Rietveld-XRD determination [16]. Up to 16% of the cement matrix is X-ray amorphous and does not contribute to the diffractogram [17]. The method normalizes the concentrations to 100%, ignoring the amorphous content, as well as traces, sulfates and hydrates whenever they occur below the XRD limit of detection. For that reason Rietveld-XRD mass balance for $SO_3$, $H_2O$, $K_2O$ and $Na_2O$ cannot be compared with known composition. The XRD sample preparation stage and long counting times during measurement result in low sample throughput. Although it is technically possible to equip an XRD instrument with a fast detector, but the additional cost (not negligible) might offset such an interest. Much progress has been accomplished in Rietveld-XRD phase quantification of various materials. Information obtained from Rietveld-XRD analysis is often unique and invaluable. However, the Rietveld-XRD method applied to cement has also its drawbacks as the method's potential to generate accurate output data is limited.

One of the most important operational advantages of C$^{em}$Quant over other methods is its ease of use, and high speed of execution. For example, it takes mere seconds to execute calculations for ten Portland cement samples using a typical PC computer. Only limited experience in chemistry or computer knowledge is required from operator. C$^{em}$Quant's accuracy approaches optical microscopy or Rietveld-XRD, and in very many instances surpasses them. Most plants are already equipped with efficient and reliable X-ray fluorescence spectrometers capable of accurately analyzing all major and minor elemental constituents with typical relative error below 1% [18-21]. One of the most important benefits resulting from a general use of C$^{em}$Quant would be a simplification of the existing analytical structures. At present, it takes XRF, XRD, DSC, TGA and also wet chemistry to carry the analytical load at various process stages. Using C$^{em}$Quant, a need to employ XRD and DSC would be much reduced. Also, use of wet chemistry could be greatly downsized. This means smaller laboratories, staff, investment and operating costs. The obvious advantages involve: gain in productivity and speed of phase analysis, efficiency, economy, uniformity (same results can be generated anywhere using the same input data), accuracy, reliability and independence. For example, in one of the cement plants in Quebec C$^{em}$Quant helps control cement grinding process using an XRF and a simple muffle furnace as the input data source. C$^{em}$Quant can also be considered as a quality control tool because it does allow calculation of process parameters. Hence, C$^{em}$Quant offers a cost-effective, reliable and attractive alternative to Rietveld based XRD methods.

## References

[1] B. Feret, C.F. Feret, C$^{em}$Quant software – Mathematical modeling in quantitative phase analysis of Portland cement, Cem Concr Res 29 (1999) 1627-1633

[2] H. F. W. Taylor, Cement chemistry, 2nd edition, Thomas Telford, London, 1997

[3] F. Kimmerle, F. Feret, B. Feret, BQUANT: cost-effective calculations of bauxite mineralogy, Light Metals (1997) 9-16

[4] D.L. Kantro, L.E. Copeland, C.H. Weise and S. Brunauer, Quantitative determination of the major phases in Portland cements by X-ray diffraction methods, J. PCA (Portland Cement Assoc.), Res. Develop. Lab. Vol. 6 (1), 1964, 20-40

[5] K. Binder, Applications of the Monte Carlo method in statistical physics, Springer Verlag, Berlin, 1987

[6] Brammer Standard Company Inc. Catalog, www.brammerstandard.com

[7] ASTM C150-04a Standard Specification for Portland Cement

[8] P. Stutzman, S. Leigh, Phase Composition Analysis of the NIST Reference Clinkers by Optical Microscopy and X-ray Powder Diffraction, NIST Technical Note 1441

[9] J.C. Taylor, Hinczak, I., Matulis, C.E., Powder Diffraction, vol. 15 (2000), pp. 7 - 18

[10] Accurate Quantitative Rietveld analysis with TOPAS in the cement industry, BRUKER Advanced X-ray Solutions, LAB Report XRD 33

[11] R. Smidt, A. Kern, Quantitative XRD Phase Analysis, World Cement, February 2001

[12] N. Lundgaard, E.S. Jons, F.L. Smidth, Quantitative Rietveld XRD Analysis, World Cement, April 2003

[13] Accurate Quantitative phase analysis of sulphates and calcite in Portland cement, BRUKER Advanced X-ray Solutions, LAB Report XRD 46

[14] G. Walenta, T. Füllmann, M. Gimenez, Quantitative Rietveld analysis of cement and clinker, International Cement Review, June 2001
[15] Evaluating properties of blended cements for concrete pavements, Iowa State University, Final Report, December 2003
[16] H.W. Meyer, J. Neubauer, S. Malovrh, Neue Qualitätssicherung mit standard-freier Klinkerphasenbestimmung nach der Rietveld-Verfeinerung im Einsatz, ZKG International, Nr. 3, 1998, pp. 152-162
[17] P. Man Suherman et al., Determination of amorphous phase levels in Portland cement clinker, Powder Diffraction, 17 (3), September 2002, pp. 178-185
[18] B.J. Price, Process control elemental analysis of cement-making materials using automated XRF spectrometers, World Cement, Vol. 17, No. 4, 1986
[19] J.A. Anzelmo, B.W. Boyer, ASTM C-114 rapid method qualification of pressed powders and fused beads by X-ray fluorescence spectrometry, World Cement, Vol. 18, No. 8, (1987)
[20] S.H. Babikian, Raw materials analysis by XRF in the cement industry, in: Advances in X-Ray Analysis, Vol. 36, Plenum Press, New York, 1993, pp. 139
[21] R.R. Fleming, J.D. Jefferson, Magnesium analysis with a low cost EDXRF cement analyzer, World Cement Research and Development, 1995, pp. 60

## Acknowledgements

We would like to acknowledge J-P. Gagnon from Corporation Scientifique Claisse and F. Slim and S. Vallerand from Ciment Quebec for very valuable technical discussions leading to improvement of the C$^{em}$Quant software.